SCIENTIFIC REPORTS

OPEN

SUBJECT AREAS:
ELECTRONIC MATERIALS AND DEVICES
INORGANIC CHEMISTRY
MATERIALS CHEMISTRY
METHODS

Received
21 June 2011

Accepted
5 September 2011

Published
19 September 2011

Correspondence and requests for materials should be addressed to N.D. (Natalia.Dubrovinskaia@uni-bayreuth.de)

Experimental pressure-temperature phase diagram of boron: resolving the long-standing enigma

Gleb Parakhonskiy[1,2], Natalia Dubrovinskaia[2], Elena Bykova[1,2], Richard Wirth[3] & Leonid Dubrovinsky[1]

[1]Bayerisches Geoinstitut, Universität Bayreuth, D-95440 Bayreuth, Germany, [2]Materialphysik und Technologie, Lehrstuhl für Kristallographie, Physikalisches Institut, Universität Bayreuth, D-95440 Bayreuth, Germany, [3]GeoForschungsZentrum Potsdam, Experimental Geochemistry and Mineral Physics, 14473 Potsdam, Germany.

Boron, discovered as an element in 1808 and produced in pure form in 1909, has still remained the last elemental material, having stable natural isotopes, with the ground state crystal phase to be unknown. It has been a subject of long-standing controversy, if α-B or β-B is the thermodynamically stable phase at ambient pressure and temperature. In the present work this enigma has been resolved based on the α-B-to- β-B phase boundary line which we experimentally established in the pressure interval of ~4 GPa to 8 GPa and linearly extrapolated down to ambient pressure. In a series of high pressure high temperature experiments we synthesised single crystals of the three boron phases (α-B, β-B, and γ-B) and provided evidence of higher thermodynamic stability of α-B. Our work opens a way for reproducible synthesis of α-boron, an optically transparent direct band gap semiconductor with very high hardness, thermal and chemical stability.

Boron does not exist in nature as a pure elemental phase because of its extreme chemical activity but, being utilised in compounds it plays an important role in human activities since antiquity[1]. Boron compounds are widely used as engineering materials (dielectrics, B-doped semiconductors), superhard materials (cBN, boron carbide), reinforcing chemical additives, for example, for obtaining special glass or corrosion- or heat-resistant alloys)[2], and superconducting materials (ex., MgB_2)[3] . Surprisingly, despite centuries of application and decades of intensive studies of boron compounds, elemental boron still remains in focus of wide scientific interest due to its enigmatic properties (largely unknown phase diagram[4–7], pressure induced metallization and superconductivity[8], formation of unusual chemical bonds[9] and potential technological applications (exceptional chemical stability combined with very high hardness and interesting semiconducting and optical properties[5,10].

Among elemental boron polymorphs, only α-rhombohedral (α-B), β-rhombohedral (β-B), and γ-orthorhombic boron (γ-B) have been currently established as pure phases[4]. They can be synthesised as single crystals at high pressures and high temperatures and preserved at ambient conditions[4, 11–14]. Building blocks of all these polymorphs are quasi-molecular B_{12} icosahedra arranged in the structures of different complexity. Among them β-B has the most complex structure, whose details should yet be clarified by further studies. The presence of not fully occupied positions and probably interstitial atoms allow characterising the structure of β-B as a defect one[7,15,16]. The γ-B consists of covalently bonded B_{12} icosahedra in a distorted cubic closest packing with B_2 dumbbells placed at the octahedral sites[5,9]. α-B has the simplest structure with only 12 atoms per a unit cell, where B_{12} icosahedra are arranged in a distorted cubic closest packing[17].

Relative stability of α-B and β-B at ambient conditions remains a puzzle. The β-B crystallizes from melt at ambient pressure and can be also produced by different chemical methods including vapour deposition[18,19]. The α-B was crystallized from a variety of metallic solvents in the middle of 1960s[20], but later the technology of producing the pure crystalline phase was lost[4] and only recently high-pressure synthesis of α-B single crystals was reported[14]. On heating at ambient pressure at temperatures above ~1500 K α-B slowly transforms to β-B and it means that a stable high-temperature form of boron is the β-phase. The fact that β-B can not be transformed to α-B at ambient pressure may indicate that α-form is metastable[21]. In this respect, although α-B is completely ordered, its relative structural simplicity does not make it self-evident that α-B is more stable compared to β-B at ambient conditions. Slow kinetics of transformations (i.e. large kinetic barriers) and/or high melting temperature of boron have possibly prevented accurate measurements by unambiguous techniques, such as calorimetry[22].

Theoreticians do not have consensus on the problem of relative stability of α-B and β-B polymorphs. Using density-functional (DFT) calculations Masaga et al. and Shirai et al.[6,23] studied ground-state and thermodynamic

properties (including the effect of atomic disorder and phonons) of α- and β-B and found that at zero temperature α-B is more stable than β-B. That agrees with the conclusion of Shang et al.[24], who considered defect free α- and β-B using first-principle quasi-harmonic phonon calculations. By considering the phonon contribution as the major source of the temperature dependence of the free energy, Masaga et al.[6] obtained 970 K as the transition temperature of α-to-β boron. This is at odds with conclusions of van Setten et al.[7], who introduced the quantum mechanical zero-point vibrational energy as a mechanism to stabilize β-B at absolute zero temperature and made β-B in their DFT calculations the ground state of elemental boron. Moreover, investigations indicate that it is possible to find an arrangement of partially occupied states in β-boron that also increase its stability with respect to the α-phase[7,15,22,25]. Ogitsu et al.[22,25], using lattice model Monte Carlo techniques combined with *ab initio* calculations, found that boron could be a frustrated system and a series of β-boron structures, nearly degenerate in energy, may be stabilized by a macroscopic amount of intrinsic defects. According to Ogitsu et al.[22,25], defects are responsible not only for entropic effects but also for a reduction in internal energy making β-B more stable than α-B at zero temperature. Thus, if the β-B phase happens to be the ground state, the presence of geometrical frustration will lead to an exotic thermodynamic property in the vicinity of zero temperature that would be very unusual for a pure elemental material.

In the present work we report the results of systematic experimental exploration of the pressure-temperature (PT) phase diagram of boron at pressures of 3 GPa to 14 GPa and temperatures of 1073 to 2423 K aimed at establishing phase boundaries and resolving the long-standing problem regarding relative stability of the α- and β-B phases.

Results

Boron phases. In order to experimentally constrain relations between α-, β-, and γ-boron phases we performed more than 30 experiments in a multi-anvil apparatus (Fig. 1, Table 1, see also Methods below). In all experiments a boron source (commercially available polycrystalline high purity (99.9995%) β-B, see Methods Summary) was enclosed into a metallic (Au or Pt) capsule with or without addition of a Pt powder and treated at various high-pressure high-temperature (HPHT) conditions. Every trial aimed at establishing the phases that can be crystallised from melt or by solid-solid phase transformation of the precursor. Recovered samples were analysed by scanning electron microscopy and electron microprobe for chemical purity, X-ray diffraction and Raman spectroscopy for phase composition, and some samples were studied by TEM for characterising their microstructure (Methods Summary).

An image of a cross-section of a typical sample chamber recovered after experiment at 7 GPa and 1573 K is shown in Fig. 2. As seen, single crystals of the boron phase are embedded into the matrix of solidified melt of platinum and platinum borides that form in all experiments at temperatures above eutectic.

Dependent on the pressure-temperature conditions, the experiments resulted in formation of the following pure boron phases:

(1) *Re-crystallised β-B*, which is different from the precursor polycrystalline β-B. It forms black or slightly reddish in thin sections single crystals of an irregular or sometimes hexagonal shape (Fig. 1), gives a typical for single crystals diffraction pattern consisting of spots (Fig. 3) (space group R*3(-)m*, a= 10.965(2) Å, c= 23.859(4) Å). Its Raman spectrum is distinctly different from that of the precursor and characterised by much sharper peaks compared to the latter (Fig. 4);

(2) *γ-B*, which appears as purple elongated prismatic crystals, gives the characteristic strong Raman spectra (Figs. 1, 4) and the X-ray diffraction pattern (space group P*nnm*, a=5.0576(4) Å, b=5.6245(8) Å, c=6.9884(10) Å). This material is identical to that described in our previous works[5,9,26].

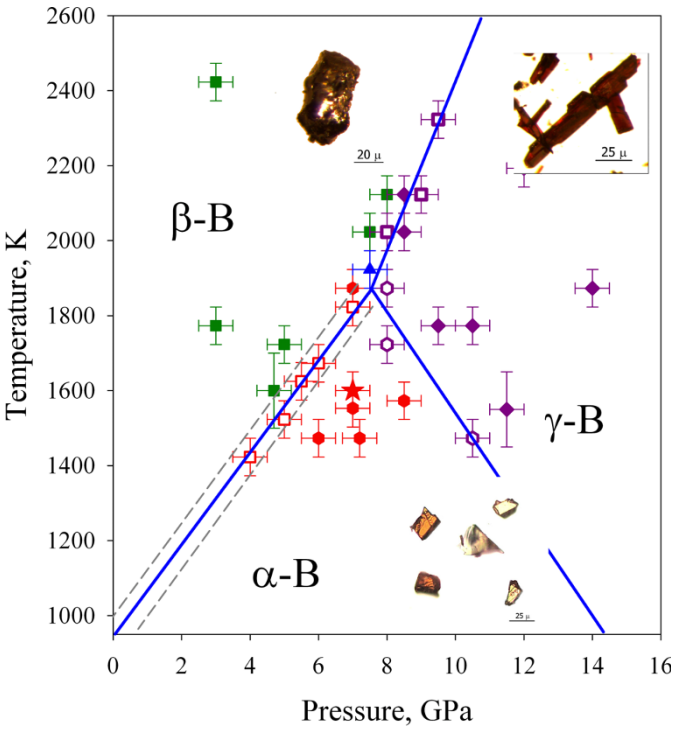

Figure 1 | Pressure-temperature phase diagram of boron. PT conditions at which crystallisation of various boron phases occurred are marked by different signs: green squares – β-boron; purple diamonds – γ-boron; red hexagons – α-boron; open red squares – α- and β-boron; open purple squares – β- and γ-boron; open purple hexagons – α- and γ-boron; blue triangle – α-, β-, and γ-boron; the red star marks the conditions of the multi-anvil experiment which led to the solid-solid β-to-α-B phase transition; continues blue lines show apparent phase boundaries. The linear regression of the experimental points gives the following equation for the α/β phase boundary: T(K)= 933(20) + 124(4)*P(GPa) (standard deviations are given in brackets). The dashed lines show the upper and lower limits in the position of the α/β phase boundary. They are drawn taking into account error bars provided. The statistical uncertainty interval obtained by linear regression of five available data points lies within the limits shown by the dashed lines. The inserts present images of synthesized crystals of α-, β-, and γ-boron.

(3) *α-B*. It forms single crystals of semi-transparent orange-red colour and relatively isometric shape (Fig. 1,2). Like other boron phases, α-B is easily identified by the Raman spectrum[14,27] (Fig. 4) and X-ray diffraction (space group R*3(-)m*, 4.9065(4) Å, 12.5658(5) Å).

The SEM (EDX), microprobe (WDX), and EELS data have shown that boron phases obtained from crystalline β-boron powders are not contaminated independently on the type of the capsule material or pressure-temperature conditions (Fig. 5). SEM images of the sample surfaces in backscattered electrons demonstrate homogeneity of the synthesized at HPHT boron phases. High resolution transmission electron microscopy (HRTEM) images of α-B, for example, reveal almost dislocation free regular packing of spheres (Fig. 5) with a diameter of 3.3-3.4 Å, comparable with that of a circumscribed circle around the B_{12} icosahedron (3.34 Å)[28].

Boron phase diagram. Proven chemical and phase purity of boron crystals obtained at different pressure-temperature condition creates a basis for construction of the experimental phase diagram. Different runs resulted in crystallization of one, two or even all three boron phases simultaneously (Fig. 1, Table 1) that allows defining stability

Table 1 | Summary of high-pressure high-temperature experiments on boron.

Experiment*	Starting material	Experimental conditions**				Synthesis results***
		capsule material	temperature, K	pressure, GPa	heating duration, Min	
H3161 MA	85 at.% β-B + 15 at.% Pt	Au	1473	10.5	5	α-B, γ-B
H3170 MA	85 at.% β-B + 15 at.% Pt	Au	1473	7.2	5	α-B
S4894 MA	β-B	Pt	1873	7	5	α-B
H3255 MA	β-B	Pt	1573	8.5	3	α-B
H3271 MA	β-B	Pt	1673	6	5	α-B, recrystallized β-B
H3273 MA	β-B	Pt	1473	6	5	α-B
H3286 MA	β-B	Pt	1873	8	5	α-B, γ-B
S4805 MA	85 at.% β-B + 15 at.% Pt	Au	1773	9.5	5	γ-B
H3154 MA	85 at.% β-B + 15 at.% Pt	Au	1773	10.5	5	γ-B
H3191 MA	β-B	Pt	2193	12	1	γ-B
H3244 MA	β-B	Pt	1873	14	2	γ-B
H3260 MA	β-B	Pt	1073	9.7	10	initial β-B
H3270 MA	β-B	Pt	1723	5	5	recrystallized β-B
S5068 MA	β-B	Pt	1423	4	5	α-B, recrystallized β-B
H3286 MA	β-B	Pt	1873	8	5	α-B, γ-B
H3292 MA	β-B	Pt	1573	7	5	α-B
S4979 MA	β-B	Au	1373	7	5	α-B, initial β-B
H3313 MA	β-B	Au	1823	7	5	α-B, recrystallized β-B
S4995 MA	β-B	Au	1623	7	5	α-B
H3315 MA	β-B	Pt	1523	5	5	α-B, recrystallized β-B
S5016 MA	β-B	Pt	2023	7.5	5	recrystallized β-B
S5017 MA	β-B	Pt	2123	9.0	5	γ-B, recrystallized β-B
S5046 MA	β-B	Pt	2023	8	5	γ-B, recrystallized β-B
S5053 MA	β-B	Pt	2023	8.5	5	γ-B
S5060 MA	β-B	Pt	2123	8	5	recrystallized β-B
S5061 MA	β-B	Pt	1723	8	5	α-B, γ-B
S5064 MA	β-B	Pt	1923	7.5	5	α-B, γ-B, recrystallized β-B
S5155 MA	β-B	Pt	1600	5.5	60	α-B, recrystallized β-B
A404 PC	β-B	Pt	1773	3	5	recrystallized β-B
A405 PC	β-B	Pt	2423	3	5	recrystallized β-B
DAC1	α-B	Re	1550	11.5	7	γ-B
DAC2	α-B	Re	1600	4.7	7	β-B

*MA – multi-anvil runs, PC – piston cylinder, and DAC – diamond anvil cell experiments
**Typical uncertainty in temperature is ± 50K, and 0.5 GPa in pressure.
***Platinum borides were found in all experiments at temperatures above eutectic if platinum as capsules material of component of starting mixture was used. In some experiments synthesis products contain initial non-transformed β-boron powder.

fields of the α−B, β−B, and γ− B phases. The phase boundary separating the β–B and γ-B phase stability fields agrees well with the phase relations experimentally found in our previous work[5].

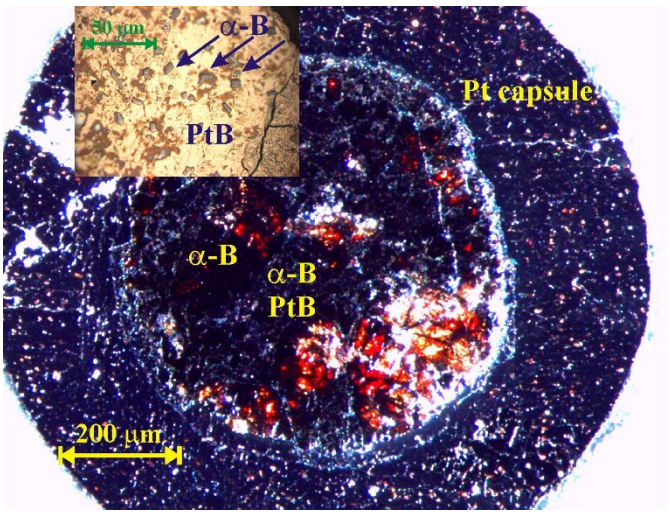

Figure 2 | Cross section of the capsule recovered after the experiment at 7 GPa and 1573 K. Bright orange-red α-boron crystals were crystallised from Pt-PtB flux. The insert shows an enlarged area containing platinum boride and small α-B crystals.

The other two phase boundaries (α−/β−B, and α−/γ− B) have not been reported so far based on experimental data. We argue that the α−B has the thermodynamic stability field, because its crystallization is controlled only by pressure and temperature conditions of the experiments independently on the type of metallic solvent (Au or Pt, Table 1). In the experiment at 5.5 GPa and 1600 K (S5155 MA, see Table 1) the sample was kept at high temperature for one hour to check if the prolonged heating can affect the result. Like in short-duration experiments at similar P-T conditions we observed two phases, recrystallized beta-boron and α-boron crystals. The α-B crystals reached up to 0.2 mm in width and up to 0.5 mm in length that is much bigger compared with those (only tens of microns in length) obtained in other experiments with a short annealing time. Growth of the α-B crystals confirms that it is a stable phase at conditions of the experiment. Observation of simultaneous crystallization of chemically pure α- and β-B (at 5 GPa and 1520 K, for example) or α- and γ-B (at 8 GPa and 1570 GPa, for example) demonstrates the existence of mono-variant points in the pressure-temperature phase diagram. The invariant (triple) point in the phase diagram could be determined by intersections of α-/β-B, α-/γ-B, and β-/γ-B boundaries. The all three lines cross at 7.6(5) GPa and 1880(50) K (Fig. 1). Indeed, at 7.5 GPa and 1920 K we observed simultaneous crystallisation of all α-, β-, and γ-boron phases (Table 1, Fig. 1).

The transition of α-to-β boron upon heating at ambient pressure was already reported in literature[20,21]. In a diamond anvil cell (DAC) experiment (see Methods Summary) we loaded two pre-synthesized

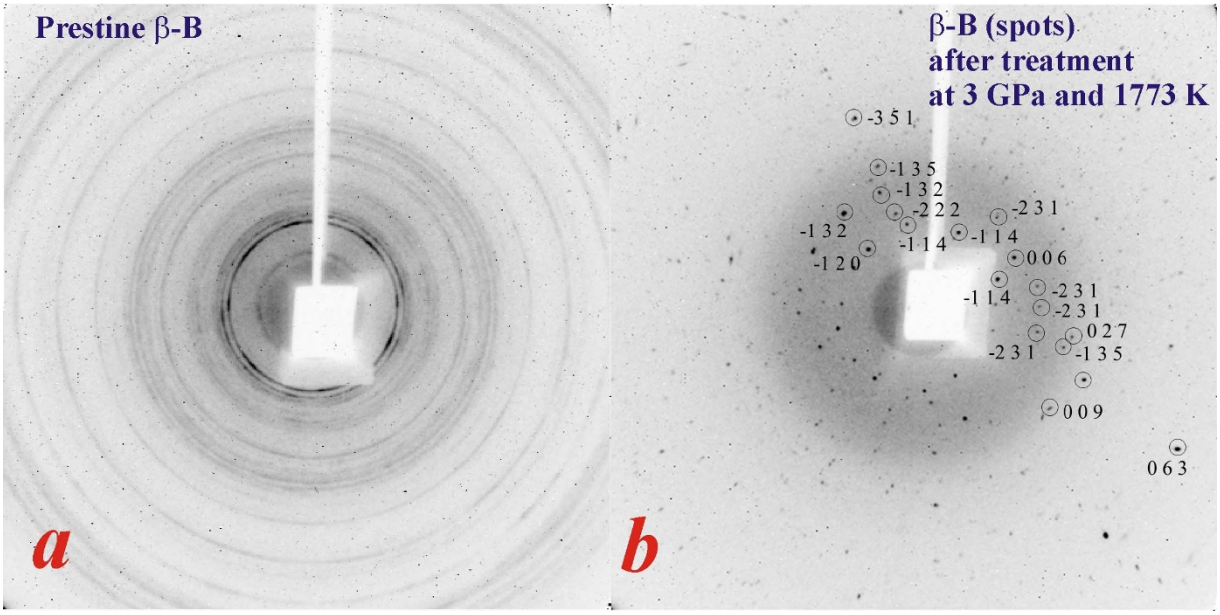

Figure 3 | 2D rotational X–ray diffraction patterns of (a) polycrystalline β–B used as starting material and (b) re-crystallized β–B single crystals consisting of diffraction spots.

α-B crystals into the sample chamber along with sodium chloride, NaCl, acting as a pressure transmitting medium and thermal insulator. One of the crystals was laser-heated at 4.7(3) GPa and 1600(100) K and another one at 11.5(5) GPa and 1550(100) K. In the first case we observed formation of β-B, while at higher pressure α-B transformed directly into the γ-phase (Fig. 6). One more MA experiment was conducted at 7 GPa and 1623 K in the Au capsule which does not dissolve boron. As in other experiments β-B was used as starting material, but in the recovered sample we found polycrystalline α-B. Direct solid-solid phase transformation of β-to-α phase proves that α-boron is a thermodynamically stable phase at certain PT conditions (Fig. 1).

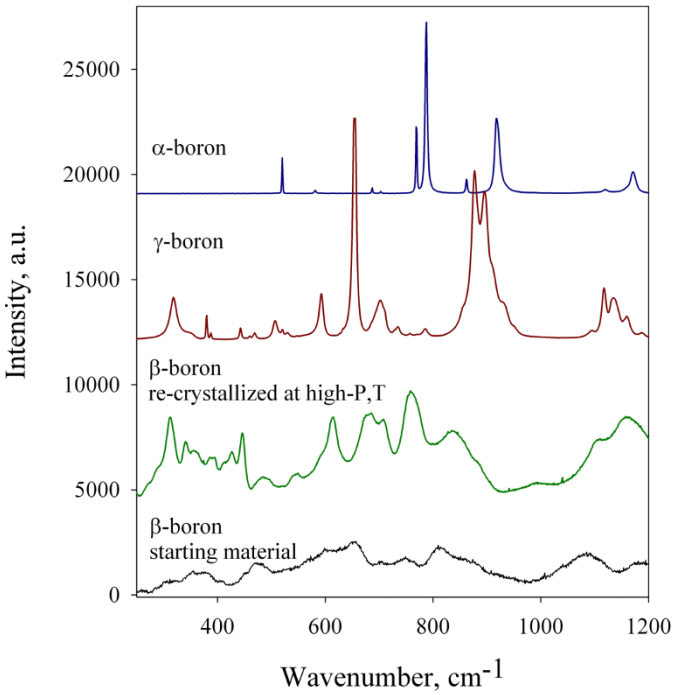

Figure 4 | Representative Raman spectra of boron phases. All spectra were collected for 10 sec except the one spectrum of starting polycrystalline β-boron collected for 60 min.

Discussion

Extrapolation of the α-/β-B boundary to ambient pressure (Fig. 1) suggests that α-boron is the thermodynamically stable low-temperature boron phase below ~933(50) K. Indeed, in 1960s and 1970s arguments were raised[20,29–33] that crystallization of small crystals of α-B from different metallic solvents (Pt, Au, Ag, Cu, Cu-Ni, etc.) at

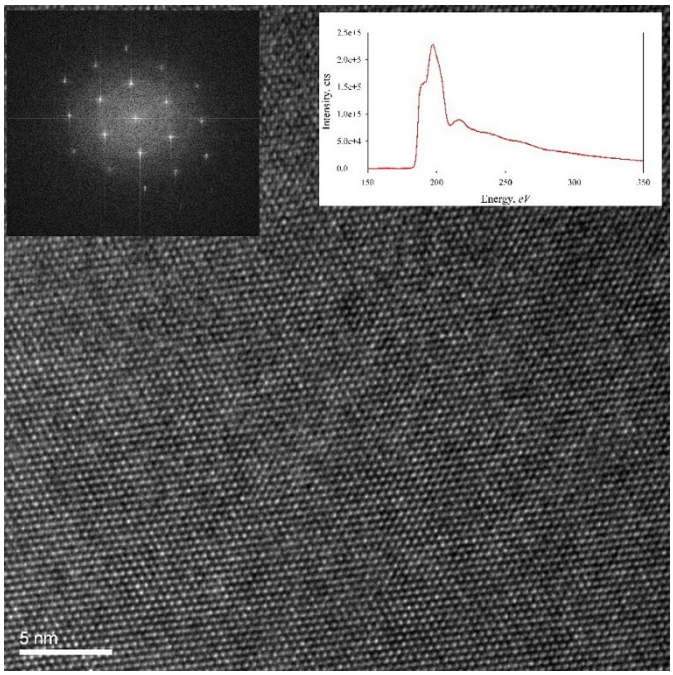

Figure 5 | High resolution TEM image of the α-boron crystal synthesized from platinum flux at 7 GPa and 1573 K. The insert in the left upper corner is a Fast Fourier Transform (FFT) pattern showing characteristic α-B reflections 4.16 Å, 4.02 Å, and 2.52 Å. The insert in the right upper corner is a core-loss EELS spectrum of the B-K edge confirming the absence of carbon contaminations at about 284 eV, the onset of the C-K edge. The spectrum has been gain-normalized and deconvoluted using the low-loss spectrum.

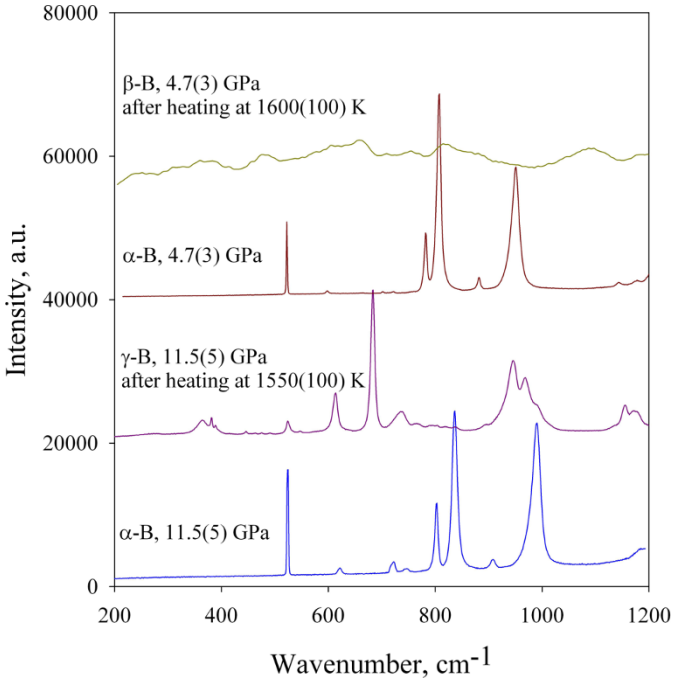

Figure 6 | Raman spectra of pre-synthesized α-B crystals taken *in situ* in a diamond anvil cell experiments at various PT conditions. From the bottom to the top: before and after laser heating at 11.5(5) GPa and 1550(100) K and at 4.7(3) GPa and 1600(100) K. At higher pressure we observed formation of γ-B, while at lower pressure α-B transformed directly in to the β-phase. (NaCl in the DAC experiments was used as a pressure transmitting medium and a thermal insulator.)

temperature around 1100–1200 K may indicate stability of the α-polymorph at temperatures below these values. However, inability to grow larger crystals of α-B, its crystallization simultaneously with the β-form, and failure to transform β-B into the α-phase or to synthesize α-B from an amorphous boron precursor supported arguments that α-B may be just a metastable, or even monotropic, form of boron. In our experiments at appropriate pressure-temperature conditions (Fig. 1) α-B crystals grow at the expense of β-B and in some runs (Table 1) all starting β-boron transforms into the α-phase. Moreover, we observed direct transformation of β-B into α-B. All mentioned observations prove that α-boron is a thermodynamically stable phase. Previously reported difficulties and even failure to synthesize α-B at ambient pressure could be explained based on the phase diagram we have experimentally constructed (Fig. 1): α-B is stable below about 1000 K and strictly speaking, should not crystallize from metallic fluxes with the eutectic point at temperature above ~1100 K. However, according to the Ostwald step rule at conditions not far from equilibrium not the most stable but the least stable polymorph that crystallizes first[34], so that α-B may appear if a boron-rich metallic flux solidified at relatively low temperature[20]. Transformation of β-B or amorphous boron into the α-phase requires very significant rearrangement and/or rupture of B_{12} icosahedra. It is impossible to activate such a rearrangement at relatively low temperatures (below 1000 K) in the field of stability of α-B. With a pressure increase the temperature stability field of α-boron increases and, as we demonstrated in an MA experiment, it becomes possible to realize the direct β-to-α-B transition.

Theoretical works[7,15,22,25] suggesting that β-B is the ground state of boron are not supported by our experimental results. The phase diagram drawn by Oganov et al.[35] is schematic and based on only a few experimental points related to the HPHT synthesis conditions of β-B. The authors[35] sketched the α-/β-B phase boundary in accordance with the theoretical data of van Setten et al.[7] and consequently suggested that β-B is stable down to 0 K at ambient pressure at odds with our conclusions. Combining *ab initio* pseudopotential calculations and some experimental data (Grüneisen parameters, particularly), Masaga et al.[6] and Shirai et al.[23] estimated the phase boundary between α- and β-B phases and apparently found that α-B is more stable below about 1000 K, in good agreement with our experimental results. However, these authors[6,23] calculated total energy of β-B using an ideal, defects free structural model which contradicts available experimental crystallographic data. Such a simplification of the structure of β-B in calculations could result in "underestimating" β-boron stability compared to other calculations[7]; i.e. the agreement with the experimental results could be reached just by chance, because indeed, according to Refs. 7, 15, 22, and 25 structural defects in β-B play key role in stabilization of the phase. Thus, our results call for further detailed theoretical investigations related to stability of boron polymorphs.

Boron has been for a long time known as prospective material[4,5] for numerous applications. α-boron demonstrates a truly spectacular combination of properties – it is a direct band gap semiconductor (with the reported band gap of 2.0 eV (Ref. 36), 2.4 eV (Ref. 37), or 2.15(2) eV as derived by us from EELS data), has a very high hardness (we measured the Vickers hardness of 38(2) GPa on polycrystalline aggregates), thermally and chemically highly resistive, and quite light (the density of α-B is 2.46 g/cm^3 vs 4.89 g/cm^3 of CdS or 6.11 g/cm^3 of GaN having comparable band gaps). Such properties may make α-B material of choice in many industrial semiconductors applications, and, especially, as a working element of solar cells with high efficiency of sun light conversion into electrical power. So far research and development on potential applications of α-boron were hindered by concerns of its thermodynamic instability and the absence of a reliable way of synthesis of single crystals. A phase diagram, as a projection of the fundamental property diagram, allows materials scientist indirect use of thermodynamics[38]. It can be utilized to understand materials behaviour and propose optimal ways of their synthesis. The phase diagram of boron (Fig. 1) shows that α-B is not only thermodynamically stable phase in a large pressure-temperature range, but it also can be reproducibly synthesized[14] at conditions readily accessible by modern industry for large-scale production (like synthetic diamonds, for example).

Summarising, our serial exploration of the pressure-temperature field using the large volume press synthesis technique resulted in establishing the phase diagram of boron in the pressure interval of 3 GPa to 14 GPa at temperatures between 1073 K and 2423 K. Based on our experimental data and linear extrapolation of the α/β phase boundary down to ambient pressure we could resolve a long-standing controversy on the ground state of boron in favour of the α−B phase.

Methods

Polycrystalline β-boron (purity of 99.9995 at. %, grain size of <1000 microns), purchased from *Chempur Inc.*, was used as a boron source material.

High-pressure techniques. Experiments in multianvil apparatuses were conducted in installed at BGI 1000-ton (Hymag) and 1200-ton (Sumitomo) hydraulic presses[39]. The Kawai-type multi-anvil system employs six tool-steel outer-anvils and eight tungsten carbide cubic inner-anvils to focus an applied load on an octahedral high-pressure chamber formed as a result of corner truncations on the inner-anvils. By varying the corner truncation size of the inner-anvils, various sample-pressure ranges can be attained. An octahedron made of magnesium oxide that matches the pressure chamber was used as a pressure medium. In our experiments 18/11 (the edge-length of an octahedron /anvil truncation edge-length, in millimeters) assemblies for pressures of 7–11 GPa and 25/15 assemblies for pressures of 5–8 GPa were used. Although an indubitable advantage of using large assemblies is the increase of the amount of synthesized material, reaching highest temperatures in big assemblies is more difficult. Temperature in our experiments was increased stepwise with a speed of about 80 K/min. Duration of heating was 5 or 3 minutes. Then the samples were either gradually cooled with a speed ~10 K/min, or quenched. "Pressure in chamber" vs "hydraulic oil pressure" in experiments was calibrated by observations of phase transitions in standard materials, and temperature determined using $W_3Re/W_{25}Re$ thermocouple. Uncertainties estimated in pressure 0.5 GPa and in temperature 50 K.

Experiments at pressures below 4 GPa were conducted using an end-loaded piston-cylinder type apparatus[40]. The sample material was loaded into 6 mm diameter, 13 mm long Pt capsules (sample area 3 mm diameter, 6 mm long) which were placed into ½ inch talc-pyrex sample assemblies. These sample assemblies contained an internal, tapered, graphite resistance furnace to ensure minimal temperature gradients along the length of the capsule. Temperature gradients are estimated to be less than 25°C for the experimental conditions used. Pressure was calibrated against the quartz-coesite and kyanite-sillimanite transitions, as well as the melting point of diopside, and pressures are considered accurate to within less than ± 5% of the stated value. Temperatures were measured with a Pt-Pt10%Rh thermocouple. Run pressures and temperatures were continually monitored and maintained for the duration of the runs. Experiments were quenched isobarically by turning off power to the heating circuit.

Diamond anvil cell experiments we conducted using diamond anvils with the culet diameter of 300 μm . Pre-synthesized α-B and NaCl (used as a pressure medium and thermal insulating material) were loaded into the pressure chamber in the Re gasket preindented to about 45 μm thickness with the hole of 125 μm in diameter. Several ruby chips were placed into the sample chamber for pressure measurements. For double-side laser heating we employed two UniHead systems installed at BGI[41]. The size of the laser beam was of about 30 μm in diameter with a temperature variation of ±50 K within the beam. The heating duration was about 5 minutes. Temperature was measured by means of multiwavelength spectroradiometry.

Analytical techniques. For the phase identification, selection of single crystals, and preliminary structural analysis a high-brilliance Rigaku diffractometer (Mo Kα radiation) equipped with Osmic focusing X-ray optics and Bruker Apex CCD detector was used. The diffraction patterns were processed using Fit2D software.

A LabRam spectrometer (with a resolution of 2 cm^{-1}), a He–Ne laser (632.8 nm) with a power of 15 mW for excitation, and a 50× objective were used for the Raman scattering experiments.

The morphology and chemical composition of the synthesized samples of single crystals were studied by means of the scanning electron microscopy (SEM) (LEO-1530). Chemical purity of the samples was confirmed using WDX microprobe analysis (JEOL JXA-8200; focused beam; 20 keV, 20 nA).

Electron transparent foils were prepared by focused ion beam (FIB) techniques. FIB allows preparation of site-specific TEM foils with typical dimensions of 15–20 μm wide, by approximately 10 μm high and approx. 0.150 μm thick[42].

TEM investigations were performed with a TECNAI F20 XTWIN transmission electron microscope operating at 200 kV with a field emission gun electron source. The TEM is equipped with a Gatan Tridiem™filter, an EDAX Genesis™ X-ray analyzer with ultra thin window and a Fishione high angle annular dark field detector (HAADF). The Tridiem filter was used for the acquisition of energy-filtered images applying a 20 eV window to the zero loss peak. EEL spectra were acquired with a dispersion of 0.1 eV/channel and an entrance aperture of 2mm. The resolution of the filter was 0.9 eV at half width, at full maximum of the zero loss peak. Acquisition time was 1 second. Spectra of the different K-edges (B, C, N, O) were acquired in diffraction mode with a camera length of 770 mm. Spectra processing (background subtraction, removal of plural scattering, quantification) was performed using the DigitalMicrograph software package. EDX spectra were usually acquired in the scanning transmission mode (STEM) using the TIATM software package of the TEM. Significant mass loss during analysis was avoided by scanning the beam in a preselected window (20 × 20 nm or larger). Spot size was approx. 1 nm, and acquisition time 60 seconds at an average count rate of 60 – 80 counts/second. This resulted in a counting error of about 4 –5% at a 3σ level.

1. Garrett, D. E. Borates: handbook of deposits, processing, properties, and use. *Academic Press* (1998).
2. Perkins, G. L. Boron: Compounds, Production and Application. *Nova Science Pub Inc.* (2011).
3. Braccini, V., Nardelli, D., Penco, R., Grasso, G. Development of ex situ processed MgB_2 wires and their applications to magnets. *Physica C: Superconductivity* **456**, 209–217 (2007).
4. Albert, B., Hillebrecht, H. Boron: elementary challenge for experimenters and theoreticians. *Angew. Chem. Int. Ed.* **48**, 8640–8668 (2009).
5. Zarechnaya, E.Yu., *et al*. Superhard semiconducting optically transparent high pressure phase of boron. *Phys. Rev. Lett.* **102**, 185501 (2009).
6. Masago, A., Shirai, K., Katayama-Yoshida, H. Crystal stability of α- and β-boron. *Phys. Rev. B* **73**, 104102 (2006).
7. Van Setten, M. J., Uijttewaal, M. A., de Wijs, G. A. & de Groot, R. A. Thermodynamic stability of boron: The role of defects and zero point motion. *J. Am. Chem. Soc.* **129**, 2458–2465 (2007).
8. Eremets, M. I., Struzhkin, V. V., Mao, H., Hemley, R. J. Superconductivity in boron. *Science* **293**, 272–274 (2001).
9. Mondal, S., *et al*. Electron deficient and multicenter bonds in the high-pressure γ-B28 phase of boron. *Phys. Rev. Lett.* **106**, 215502 (2011).
10. Zhou, W., Sun, H., Chen, C. Soft bond-deformaton paths in superhard gamma-boron. *Phys. Rev. Lett.* **105**, 215503 (2010).
11. Brazhkin, V. V., Taniguichi, T., Akaishi, M., Popova, S. V. Fabrication of β-boron by chemical-reaction and melt-quenching methods at high pressures. *J. Mat. Res.* **19**, 1643–1648 (2004).
12. Zarechnaya, E.Yu., Dubrovinsky, L., Dubrovinskaia, N., Filinchuk, Y., Chernyshov, D., Dmitriev, V. Growth of singlecrystals of B28 at high pressures and high temperatures. *J. Cryst. Growth* **312**, 3388–3394 (2010).
13. Zarechnaya, E.Yu., *et al.* L. Pressure-induced isostructural phase transformation in γ-B28. *Phys. Rev. B* **82**, 184111 (2010).
14. Parakhonskiy, G., Dubrovinskaia, N., Dubrovinsky, L., Mondal, S., van Smaalen, S. High pressure synthesis of single crystals of α-boron. *J. Cryst. Growth* **321**, 162–166 (2011).
15. Widom, M., Mihalcovic, M. Symmetry-broken crystal structure of elemental boron at low temperature. *Phys. Rev. B* **77**, 064113 (2008).
16. Slack, G. A., Hejna, C. I., Garbauskas, M. F., Kasper, J. S., *J. Sol. Stat. Chem.* **76**, 52–63 (1988).
17. Decker, B. F., Kasper, J. S. The crystal structure of simple rhombohedral form boron. *Acta Crys.* **12**, 503–506 (1959).
18. Cueilleron, J., Viala, J. C. The Chemical and Pyrometallurgical Purification of β-Rhombohedral Boron. *J. Less-Com. Met.*, **67**, 333–337 (1979).
19. Greenwood, N. N., in Bailar, J. C. (ed.). Comprehensive Inorganic Chemistry. *Pergamon Press, Oxford-New York* **1**, 680–689 (1973).
20. Wald, F. On the stability of the red α-rhombohedral boron modification, *Elec. Tech.* **3**, 103–108 (1970).
21. Shalamberidze, S. O., Kalandadze, G. I., Khueldze, D. E., Tsurtsumia, B. D. Production of α-rhombohedral boron by amorphous boron crystallization. *J. Sol. St. Chem.* **154**, 199–203 (2000).
22. Ogitsu, T., Gygi, F., Reed, J., Motome, Y., Schwergler, E., Galli, G. Imperfect crystal and unusual semiconductor element. *J. Am. Chem. Soc.* **131**, 1903–1909 (2009).
23. Shirai, K., Masago, A., Katayama-Yoshida, H. High-pressure properties and phase diagram of boron. *Phys. Stat. Sol. (b)* **244**, 303–308 (2007).
24. Shang, S., Wang, Y., Arroyave, R., Liu, Z.-K. Phase stability in alfa and beta-rhombohderal boron. *Phys. Rev. B.* **75**, 092101 (2007).
25. Ogitsu, T., *et al*. Geometrical frustration in an elemental solid: An Ising model to explain the defect structure of *β*-rhombohedral boron. *Phys. Rev. B* **81**, 020102R (2010).
26. Zarechnaya, E., Dubrovinskaia, N., Dubrovinsky, L. Polarized Raman spectroscopy of high pressure orthorhombic boron phase. *J. High Pressure Research* **29**, 530–535 (2009).
27. Polian, A., Ovsyannikov, S., Gauthier, M., Munsch, P., Chervin, J. C., Lemarchand, G. High pressure crystallography: from fundamental phenomena to technological applications, in: E.Boldyreva, P. Dera (Eds.). *NATO Science for Peace and Security SeriesB: Physics and Biophysics XIV, Springer, Dordrecht, Netherlands*, 241–250 (2010).
28. Zarechnaya, E. Yu., *et al*. Synthesis of an orthorhombic high pressure boron phase. *Sci. Technol. Adv. Mater.* **9**, 044209 (2008).
29. Hoard, F. L., Hughes, R. E. The chemistry of boron and its compounds. *John Wiley and Sons Inc.* 25–98 (1967).
30. Horn, F. H. "Boron" synthesis, structure, and properties. *Plenum Press Inc.* 110–115 (1960).
31. Horn, F. H., Taft, E. A., Oliver, D. W. Boron, 2, preparation, properties and applications. *Plenum Press Inc.* 231–234 (1965).
32. Niemyski, T., Zawadzki, W. Some properties of pure polycrystalline boron. *Phys. Let.* **2**, 30 (1962).
33. Wald, F., Rosenberg, J. A., Constitutional investigations in the boron-platinum system. *Trans. Met. Soc. AIME*, **233**, 796 (1965).
34. Van Santen, R. A. The Ostwald step rule, *J. Phys. Chem.*, **88**, 5768–5769 (1984)
35. Oganov, A. R., *et al*. Ionic high-pressure form of elemental boron. *Nature letters* **457**, 863–867 (2009); **460**, 292 (2009).
36. Horn, F. Some electrical and optical properties of simple rhombohedral boron. *J. Appl. Phys.* 30, 1611–1613 (1959).
37. Terauchi, M., Kawamata, Y., Tanaka, M., Takeda, M., Kimura, K. Electron energy-loss spectroscopy study of the electronic structure of α-rhombohedral boron. *J. Sol. State Chem.* **133**, 156–159 (1997).
38. Hillert, M. Phase equillibria, phase diagrams and phase transformations: their thermodynamic basis. *Cambridge Univ. Press* (2007).
39. Dubrovinskaia, N., Dubrovinsky, L., Miyajima, N., Langenhorst, F., Crichton, W. A., Dubrovinskaia, N., Dubrovinsky, L., Miyajima, N., Langenhorst, F., Crichton, W. A., Braun, H. F. High-pressure high-temperature synthesis and characterization of boron-doped diamond. *Zeitschrift für Naturforschung* **61b**, 1561–1565 (2006).
40. Dubrovinskaia, N., Dubrovinsky, L., McCammon, C. Iron-magnesium alloying at high pressures and temperatures. *J. of Physics: Condensed Matter*, **16**, S1143–S1150 (2004).
41. Dubrovinsky, L., *et al*. Portable laser-heating system for diamond anvil cells. *J. Synchrotron Rad.*, **16**, 737–741 (2009).
42. Wirth, R. Focused Ion Beam (FIB): A novel technology for advanced application of micro- and nanoanalysis in geosciences and applied mineralogy. *Eur. Journal Mineralogy*, **16**, 863–877 (2004).

Acknowledgements

The work was supported by the German Research Foundation (DFG) through the DFG Priority Program 1236. N.D. thanks DFG for the financial support through the Heisenberg Program.

Author Contributions

L.D. and N.D. designed research; G.P., N.D., L.D., E.B., and R.W. performed research and analyzed data; G.P., L.D. and N.D. wrote the paper.

Additional information

Competing financial interests: The authors declare no competing financial interests.

How to cite this article: Parakhonskiy, G., Dubrovinskaia, N., Bykova, E., Wirth, R. & Dubrovinsky, L. Experimental pressure-temperature phase diagram of boron: resolving the long-standing enigma. *Sci. Rep.* **1**, 96; DOI:10.1038/srep00096 (2011).